Prospects of Parallel ZTE Imaging

T. Oberhammer[1], M. Weiger[2,3], F. Hennel[3], and K. P. Pruessmann[1]
[1]Institute for Biomedical Engineering, University and ETH Zurich, Zurich, Switzerland, [2]Bruker BioSpin AG, Faellanden, Switzerland, [3]Bruker BioSpin MRI GmbH, Ettlingen, Germany

Introduction MRI of short-T_2 samples is performed efficiently with a 3D centre-out radial acquisition scheme and ultra-short echo time (UTE) [1]. Alternatively, the read gradient is switched on before the RF excitation with a large-bandwidth hard pulse, resulting in imaging with zero echo time (ZTE) and a shorter readout duration [2, 3] (Fig. 1). However, data in ZTE is only available after an initial dead time Δ due to the durations of RF pulse, send-receive switching, and digital filter build-up. The associated missing low-frequency components are restored by algebraic image reconstruction, involving finite support extrapolation based on radial acquisition oversampling [4, 5]. However, for large Δ this procedure is accompanied by noise amplification and correlation [6]. The present work aims to explore parallel imaging (PI) [7-9] as a remedy to this issue. Complementing gradient encoding by sensitivity encoding with a receiver array, PI is a generic way of addressing sampling gaps in *k*-space and was thus hypothesised to significantly expand the range of gaps and hence of bandwidths that can be handled in ZTE.

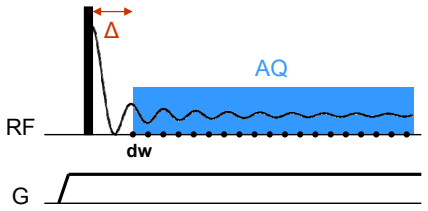

Figure 1: *Acquisition scheme for ZTE imaging with dwell time* dw *and time* Δ.

Methods For algebraic image reconstruction [5, 9] of single-coil ZTE data an encoding matrix **E** is generated, accommodating the harmonic terms related to gradient encoding. **E** differs from a standard discrete Fourier transform (DFT) in that the missing low-*k* encoding functions are excluded and additional entries reflect the acquisition oversampling. The reconstruction matrix **F** is then obtained as the pseudoinverse $\mathbf{E}^{+}$. With PI, also the coil sensitivities are included into the now expanded $\mathbf{E}_{PI}$. For comparison, images are also created for each coil separately using the original **E**, and then combined by complex weighting according to Roemer [10]. The resulting image noise is described by the noise covariance matrix $\mathbf{X} = \mathbf{F}\Psi\mathbf{F}^{H}$, where **Ψ** is the noise covariance of the input data. The diagonal of **X** is the noise variance of each image pixel. It is uniform in the DFT case while the non-diagonal elements are zero. The latter are easier to interpret after normalisation according to $X'(i,j) = X(i,j)/\sqrt{X(i,i)}/\sqrt{X(j,j)}$, where **X'** provides the noise correlation between all pixels.
In 3D ZTE reconstruction without PI, the algebraic part is used to provide 1D radial projection data, which are then joined by regridding to form a 3D image. However, due to the 3D nature of the involved coil sensitivities, 3D ZTE reconstruction with PI must be handled as a single inversion problem. Recognising the computational burden of such an approach, the initial investigation of the present study was restricted to 1D and 2D ZTE imaging.

Results Using simulations, the standard ZTE case with one uniform coil and oversampling factor ov = 2 was compared with three reconstructions from two-coil acquisitions: Roemer with ov = 2, PI with ov = 2, and PI without oversampling (ov = 1). The first column of Fig. 2 shows the 1D image noise covariance which is normalised with respect to the standard DFT case. With one-coil, a strongly increased covariance as well as strong correlations are observed [6]. This kind of noise amplification is reflected by the reconstructed 1D box, where different input noise in the subsequent scans results in changing low-frequency, artefact-like shapes superimposed onto the object. Using two coils instead and a Roemer combination results in a similar degree of noise enhancement but a correlation pattern that reflects the modified geometry. However, using PI reconstruction considerably reduces the covariance as well as the correlated noise in the 1D images, while the correlation pattern is spread - as initially - across the full FOV. Notably, with PI it is even possible to work without oversampling, resulting in an only slightly worsened situation. Consistent results are observed for the simulated 2D axial images obtained directly from algebraic reconstruction without the use of regridding. Without PI, correlated low-frequency noise is observed which appears as an artefact in the phantom image. With PI, the correlated part of the noise is largely eliminated, and primarily uncorrelated noise is observed at locations of low coil sensitivity both with and without oversampling.

Conclusion It has been found that the noise behaviour of ZTE reconstruction is considerably improved by parallel imaging. The improvements can be utilised to enable larger dead times, allowing in turn acquisitions with larger bandwidth for imaging samples with even shorter T_2. However, PI-ZTE with real data needs expansion of the reconstruction to 3D, requiring appropriate methods for handling the associated large inversion problem. One approach would be using iterative algorithms, thus reducing the memory and computational burden. In a more specific attempt, a reduced support range could be used to recover the *k*-space centre, while the final reconstruction would be based on regridding. Although the above findings apply for ZTE without acceleration, the latter can directly be included into the described concepts. A further practical issue to be addressed will be the determination of the coil sensitivities in short-T_2 samples.

References [1] Glover G, JMRI 2 (1992) 47 [2] Hafner S, MRM 12 (1994) 1047 [3] Weiger M, ISMRM (2010) 695 [4] Jackson J, MRM 11 (1989) 248 [5] Kuethe DO, JMR 139 (1999) 18 [6] Weiger M, submitted to ISMRM (2011) [7] Sodickson DK, MRM 38 (1997) 591 [8] Griswold MA, MRM 47 (2002) 1202 [9] Pruessmann KP, NMR Biomed 19 (2006) 288. [10] Roemer PB, MRM 16 (1990) 192

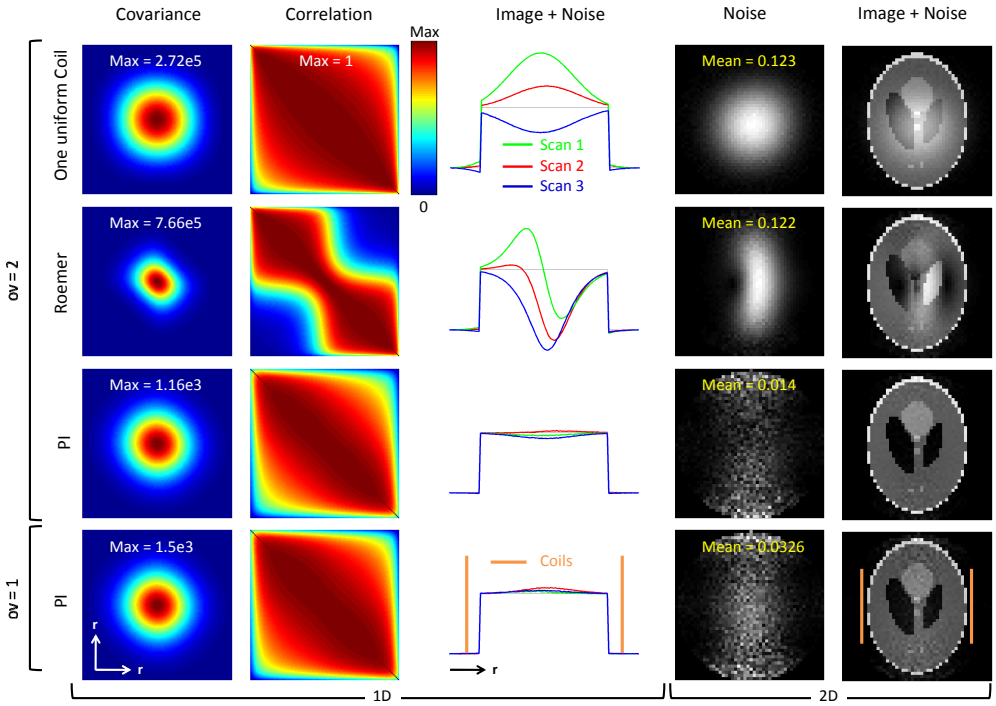

Figure 2: *ZTE imaging simulated with dead time Δ = 3 dwells, using different reconstruction approaches. For the Roemer and PI reconstructions, two circular coils with a diameter of FOV/2 were calculated using Biot-Savarts law and placed on both sides of the object in the left-right dimension. PI was performed with (ov = 2) and without (ov = 1) radial acquisition oversampling. For the 1D case (matrix 128), noise covariance and correlation matrices as well as multiple reconstructed images (real part) with different noise input in subsequent scans are shown. Identical noise is used for the different reconstruction types. For the 2D case (matrix 48^2), images reconstructed from pure noise as well as phantom images with noise are displayed.*